



Magnetic field inversions from Stokes profiles generated by MHD simulations

E. Khomenko^{1,2} and M. Collados¹

¹ Instituto de Astrofísica de Canarias, 38205, C/ Vía Láctea, s/n, Tenerife, Spain

² Main Astronomical Observatory, NAS, 03680, Kyiv, Ukraine

Abstract. We report tests of inversion methods applied to complex Stokes spectra generated by realistic MHD simulations. The average magnetic field strength of the simulations used is of 30 and 140 G, which we believe is representative of quiet solar regions. The behaviour of the Fe I at 1.56 μm and 630 nm lines is analyzed. The tests have been done with the original resolution of simulations (20 km) and also with resolution of 0".6 and 1".4 (after having conveniently degraded the images).

Key words. MHD; Sun: magnetic fields; Sun:infrared; Sun: polarization

1. Introduction

During the last decade, numerous works have dealt about the solar magnetic properties outside active regions. Since most of the solar surface is void of them, a large amount of energy may be stored there. Surprisingly, the different techniques used to analyze the observational data do not give compatible results. On the one hand, there are works based on spectropolarimetric observations in the near infrared, covering the extremely magnetically sensitive Fe I 15648 Å spectral line (with $g = 3$), and its nearby less sensitive Fe I 15652 Å line ($g = 1.53$). All the works done in this spectral region give unambiguously a predominance of magnetic fields with strengths of few hundred Gauss (Lin, 1995; Lin & Rimmele, 1999; Collados, 2001; Khomenko et al., 2003; Sánchez Almeida et al., 2003; Martínez González et al., 2006a;

Domínguez Cerdeña et al., 2006). López Ariste et al. (2006) have confirmed this result based on the study of the Stokes profiles generated by some Mn I spectral lines with a special hyperfine structure. On the other hand, studies using the Stokes profiles generated by the Fe I lines at 6301 Å ($g = 1.67$) and 6302 Å ($g = 2.5$) conclude that there is a significant percentage of strong kiloGauss fields, carrying most of the magnetic energy in these quiet areas (Sánchez Almeida & Lites, 2000; Lites, 2002; Socas - Navarro & Sánchez Almeida, 2002; Sánchez Almeida et al., 2003; Domínguez Cerdeña et al., 2003, 2006).

Despite the results seem to be strongly biased depending on the spectral region observed, the techniques used for the analyzes are also assorted. They range from simple diagnostic tools based on Stokes V amplitude ratios to the application of sophisticated inversion procedures, either assuming a Milne-Eddington approximation or a more complex atmosphere. Doubts have been casted, though,

Send offprint requests to: E. Khomenko

on all these methods, especially when applied to the weak polarization signals observed in internetwork regions (Bellot Rubio & Collados, 2003; Socas - Navarro & Sánchez Almeida, 2003; Khomenko & Collados, 2007; Martínez González et al., 2006b).

In parallel, numerical magneto-convection simulations have reached an extremely high degree of reality and, among other possibilities, give chances to emulate the different observational techniques and the various diagnostic procedures. In this contribution, we want to check the validity of inversions based on the SIR code (Ruiz Cobo & del Toro Iniesta, 1992) using Stokes profiles emerging from snapshots obtained with the MURAM code (Vögler et al., 2005) with different magnetic flux densities and spatial resolutions.

2. Data analysis

Two snapshots of average magnetic fields $\langle |B| \rangle = 30$ G and $\langle |B| \rangle = 140$ G with bipolar structure have been used in this work as representative of the quiet sun conditions. The computational domain covers $6 \times 6 \times 1.4$ Mm³ with a spatial resolution of 20 km. For each point of both snapshots, the full Stokes profiles of the two pairs of FeI lines at 630 nm and 1.56 μ m have been synthesized, as observed at disk center. All the emerging spectra have been inverted using the SIR code and the resulting model atmospheres compared to the *true* ones used for the syntheses. The inversion has been applied to the original data, with full 20 km resolution, and after degrading them to a spatial resolution of 0".6 and 1".4, thus simulating good and medium observing conditions, respectively. Both spectral regions have been treated separately, as if they were representing independent observations. The main results of these calculations are described below.

2.1. Original 20 km resolution

In this case, a single magnetic component is assumed to exist in each inverted point (*i.e.*, the filling factor is unity). Gradients in the magnetic field vector and line of sight velocity are allowed to account for the large asymmetries of

the emerging profiles. To simplify the analysis, no noise has been introduced to the resulting spectral profiles.

Figure 1 shows the maps of the retrieved magnetic field strength using the IR lines and the visible lines. For comparison, the original magnetic field strength of the simulations (with $\langle |B| \rangle = 140$ G) is also presented. All magnitudes correspond to the layer where $\log \tau = -0.4$. Even if the maps do not match exactly, the strong resemblance is apparent. The inversion process is thus capable of accurately recovering magnetic fields as weak as 50-100 G. To confirm this result, the histograms, computed over the whole surface, corresponding to the original magnetic field strengths (black), inverted using the visible lines (red) and using the IR lines (green) are displayed in the lower plot of the figure. As expected, the three distributions are almost undistinguishable.

This is not a surprising result. Since our MHD simulations do not have structures below 20 km, the assumption of unity filling factor taken for the inversions is essentially correct. Under these conditions the Stokes V amplitude, which is normally proportional to the flux, now becomes proportional to the longitudinal magnetic field component. And the same happens with the Q and U amplitudes and the transversal component. For this reason, with the full 20 km resolution, the inversion process has no difficulties in recovering the original model atmospheres, even with very weak magnetic field strengths. This is demonstrated by the example stratifications of magnetic field strength and velocities shown in Figure 2.

2.2. Reduced 0.6-arcsec resolution

After degrading the original results to a spatial resolution of 0".6, equivalent to good seeing conditions, the resulting Stokes spectra have been inverted. To make the analysis more similar to real observed data, noise with a standard deviation of 8×10^{-4} , in units of the mean continuum intensity, has been added and only those profiles with polarization amplitude larger than 4×10^{-3} have been analyzed. In such conditions, the linear polarization profiles

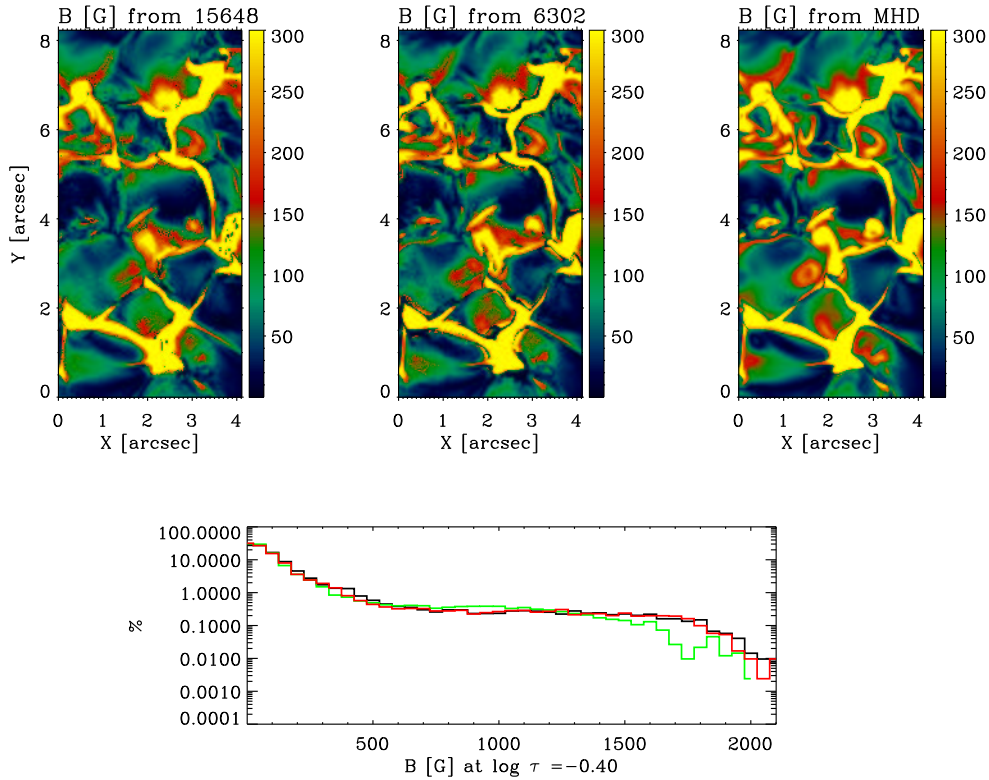


Fig. 1. Top: maps of the magnetic field strength recovered from the inversion of the IR lines (left), visible lines (middle) and the original snapshot of simulations with bi-polar magnetic field of $\langle |B| \rangle = 140$ G (right) at $\log \tau = -0.4$. The profiles are taken at their original numerical spatial resolution of 20 km. Bottom: histogram of the magnetic field strength over all the pixels. Black line - original MHD snapshot, red line - Fe I 6301, 6302 Å spectral lines, green line - Fe I 15648, 15652 Å spectral lines.

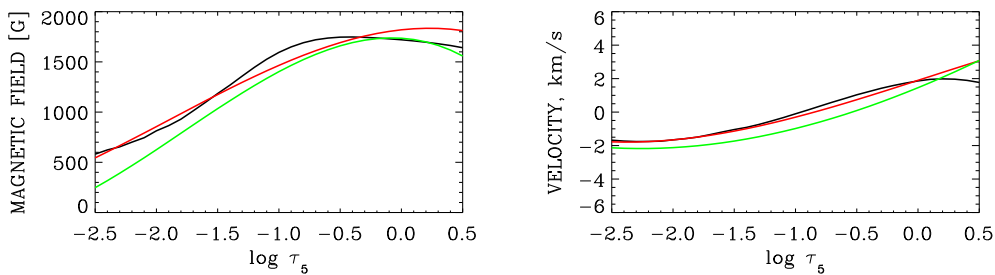


Fig. 2. Magnetic field strength and velocity stratifications of a sample point of the map: Original data (black line), retrieved stratifications using the visible lines (red line) and using the infrared lines (green line).

remain below the nose level. For this reason, only the Stokes I and V profiles have been used.

Now, the existence of one magnetic and one non-magnetic atmosphere, with different temperature stratifications, is mandatory, with

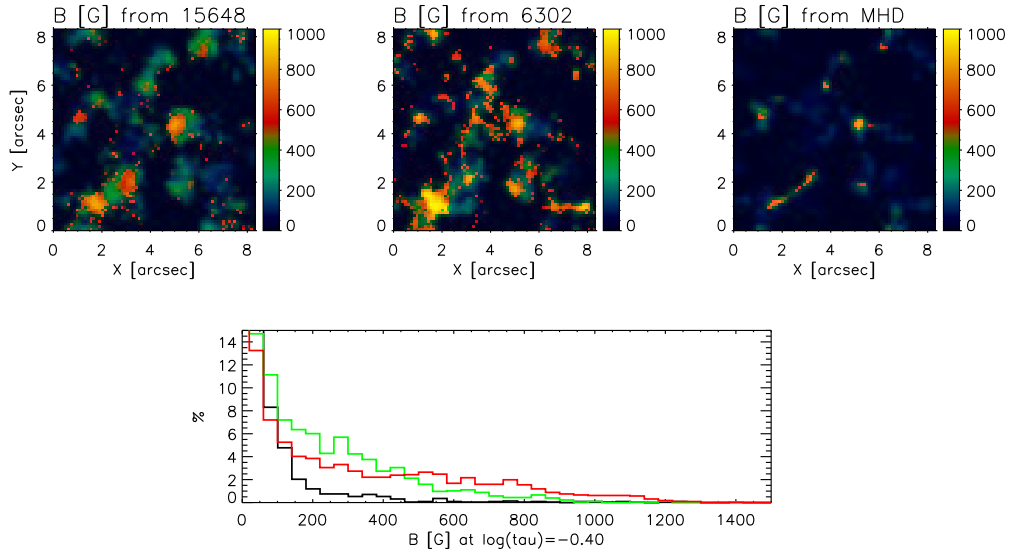


Fig. 3. Same as Fig. 1, but for a spatial resolution of 0.6 arcsec. The simulation snapshot has a bi-polar magnetic field with $\langle |B| \rangle \geq 30$ G strength.

the filling factor as a free parameter, to account for the contamination on a given point by its neighborhood. The magnetic field vector and line of sight velocity are assumed to be constant with height. In addition, free (constant with height) micro- and a macro-turbulent velocities are added.

The top panels in Fig. 3 show the resulting maps of the magnetic field strength obtained from the inversions of the infrared lines (top left panel) and the visible lines (top central panel) for the simulations with $\langle |B| \rangle \geq 30$ G. For comparison, the top right panel shows the original data at full 20 km resolution at $\log \tau = -0.4$. Ideally, it would have been better to degrade also this map. However, this is not an obvious task. A loss of resolution implies a mixture of the Stokes profiles of one point with its neighbors. With this, the corresponding magnetic fields are not mixed. Rather, each neighboring point contributes with a given weight to the observed profiles. The information is thus mixed at the level of filling factor and it is not easy to translate this information to an equivalent magnetic field strength. The

comparison of the results of the inversions with the original map can be done, though. The infrared lines recover B rather satisfactorily. The loss of resolution is apparent and each strong field feature now looks like a large spot with a size given by the imposed resolution. Even small points with an intermediate field strength of few hundred Gauss clearly show this loss of resolution. These results show that, in a degraded image, the largest magnetic fields (with largest polarization amplitudes) will dominate over their neighborhoods. The net effect is as if the degradation would have been applied directly to the magnetic field map. The results obtained with the visible lines are similar, although a little noisier. All original magnetic structures seem to have been expanded to have a size given by the spatial resolution. The visible lines have a tendency, though, to give magnetic field strengths slightly larger than the infrared ones.

The plot located in the bottom part of Fig. 3 shows the histograms of magnetic field strengths retrieved for both spectral ranges, which can be compared with the original dis-

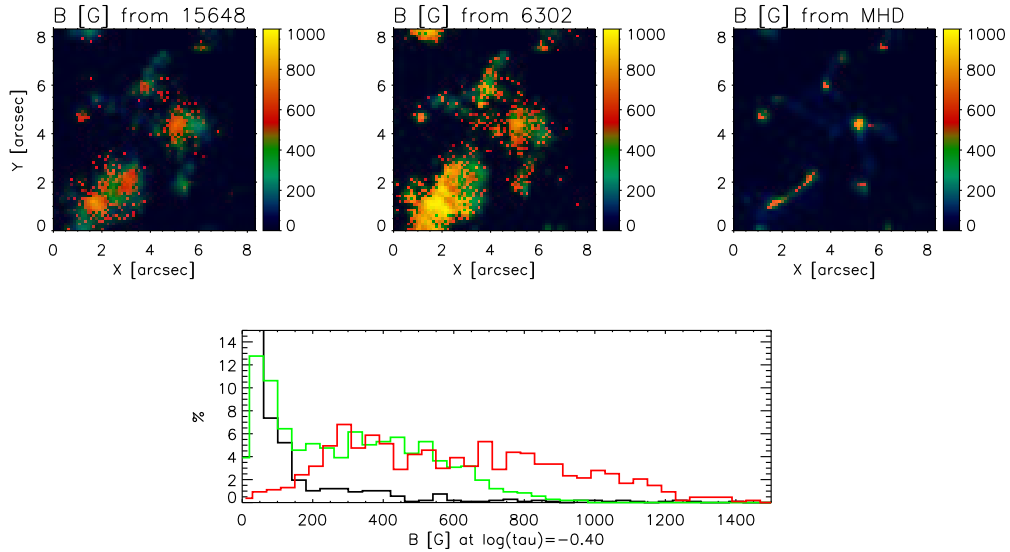


Fig. 4. Same as Fig. 3, but for a spatial resolution of 1.4 arcsec.

tribution, also displayed in the same figure. As already commented in the previous paragraph, both the visible and the infrared line inversions overestimate the presence of medium and strong magnetic field strengths, due to the expansion of the structures with the largest B induced by the loss of spatial resolution. This effect is more pronounced in the visible lines, leading to an overestimation of kiloGauss field strengths.

2.3. Reduced 1.4-arcsec resolution

The same analysis as in the previous section has been performed, but now degrading the original MHD snapshot with $|B| = 30$ Gauss to $1''.4$. The results are displayed in Fig. 4, with the same format as Figs. 1 and 3. As can be seen, the magnetic field strength map obtained from the inversion of the infrared lines still has a good quality. It has the same appearance as that with $0''.6$ resolution, except that the structures look now larger. The map obtained with the visible lines indicate now a considerable excess of strong field features. This is also ap-

parent in the histograms shown in the figure. As we understand it, the reason for this failure is the low filling factor occupied by the magnetic component in each of the pixels. Figure 5 shows the histograms of this parameter obtained from the inversion of the visible lines with both degraded cases. For $0''.6$ resolution, the magnetic component still occupies a significant fraction of all pixels analyzed. The inversion code, thus, extracts the information on the magnetic field from both I and V Stokes profiles. For $1''.4$ resolution, this is no longer the case. Filling factors with values of few percent are now retrieved. The intensity profiles do only carry information of the non-magnetic atmosphere. All the properties of the magnetic atmosphere must then be derived from Stokes V , which does not carry enough information for its accurate determination.

3. Conclusions

We have presented the results of tests of inversion methods that are frequently applied to observed Stokes spectra in order to infer the magnetic field strength. We find that an inver-

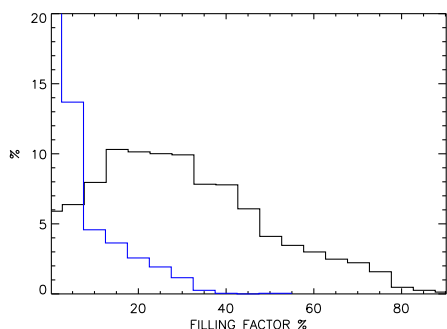


Fig. 5. Histograms of the filling factor obtained from the inversion of the FeI 6301, 6302 Å lines at the resolution of 0.6 arcsec (black line) and 1.4 arcsec (blue line).

sion applied to the Stokes profiles generated by MHD simulations at the original resolution of 20 km recovers well the original distribution of the atmospheric parameters in the case of both IR and visible lines. Both spectral regions inverted separately give results that agree between each other as well as with the original magnetic field distribution from the MHD simulations. If the MHD simulations were the Sun, the magnetic field strength could be recovered fairly well from the FeI 6301, 6302 Stokes profiles at the resolution of 0.6 arcsec, but not at 1.4 arcsec. The reason is the factor 10 difference in the filling factor. This problem is much less important in the case of the IR lines due to their larger Zeeman sensitivity.

Acknowledgements. The authors are grateful to A. Vögler for the kind permission to use the 3D model atmosphere for our study. This research was funded by the Spanish Ministerio de Educación y Ciencia through project AYA2004-05792.

References

- Bellot Rubio, L. R. & Collados, M. 2003, *A&A*, 406, 357
- Collados, M. 2001, in *Advanced solar polarimetry: Theory, observation and instrumentation*, ed. M. Sigwarth, Vol. 236 (ASP Conf. Series), 255–272
- Domínguez Cerdeña, I., Sánchez Almeida, J., & Kneer, F. 2003, *A&A*, 407, 741
- Domínguez Cerdeña, I., Sánchez Almeida, J., & Kneer, F. 2006, *ApJ*, 646, 1421
- Khomenko, E. V. & Collados, M. 2007, *ApJ*, submitted
- Khomenko, E. V., Collados, M., Solanki, S. K., Lagg, A., & Trujillo Bueno, J. 2003, *A&A*, 408, 1115
- Lin, H. 1995, *ApJ*, 446, 421
- Lin, H. & Rimmele, T. 1999, *ApJ*, 514, 448
- Lites, B. W. 2002, *ApJ*, 573, 431
- López Ariste, A., Martínez González, M. J., & Ramírez, J. 2006, *A&A*, in press
- Martínez González, M. J., Collados, M., & Ruiz Cobo, B. 2006a, in *4th Solar Polarization Workshop*, Eds.: R. Cassini & B. W. Lites, ASP Conf. Ser.
- Martínez González, M. J., Collados, M., & Ruiz Cobo, B. 2006b, *A&A*, 456, 1159
- Ruiz Cobo, B. & del Toro Iniesta, J. C. 1992, *ApJ*, 398, 375
- Sánchez Almeida, J. & Lites, B. W. 2000, *ApJ*, 532, 1215
- Sánchez Almeida, J., Domínguez Cerdeña, I., & Kneer, F. 2003, *ApJ*, 597, L177
- Socas - Navarro, H. & Sánchez Almeida, J. 2002, *ApJ*, 565, 1323
- Socas - Navarro, H. & Sánchez Almeida, J. 2003, *ApJ*, 593, 581
- Vögler, A., Shelyag, S., Schüssler, M., et al. 2005, *A&A*, 429, 335